BMC Medicine

RESEARCH

Open Access

Analysis of the prognostic efficacy of syndecan-1 for patients with ACLF and its functional role in liver regeneration

Yingli He[1,3†], Xiaoli Zhang[1†], Yichen Yao[4], Juan Li[1], Shan Fu[1], Yali Feng[1], Tianzhi Ni[1], Ruojing Wang[1], Qiao Zhang[1], Yushan Liu[1], Zhijun Liu[1], Jinfeng Liu[1], Yuan Yang[1], Yingren Zhao[1,2*] and Yalei Zhao[1,2*]

Abstract

Background Acute-on-chronic liver failure (ACLF) is a syndrome characterized by systemic inflammation with a high short-term mortality rate. Syndecan-1 (SDC-1) can independently predict the 90-day mortality of patients with septic shock. However, the role of SDC-1 in ACLF remains unknown.

Methods In this study, serum SDC-1 levels were examined in 2 cohorts, which included 174 ACLF patients. And a mouse ACLF model induced by tetrachloride, lipopolysaccharide, and D-galactosamine was established, to evaluate the effects of sulodexide and heparan sulfate (side chains of SDC-1) on ACLF in vivo.

Results Baseline serum SDC-1 levels in 101 ACLF patients (847.72, 499.79–1511.37 ng/ml) were significantly higher than in healthy controls (33.58, 27.08–43.34 ng/ml) ($P < 0.0001$). The baseline SDC-1 levels of patients who died or accepted a liver transplantation within 90 days were markedly higher than those of patients who survived ($P < 0.05$). A novel prognostic model (UIAS) based on upper gastrointestinal bleeding, INR, age, and SDC-1 was developed. The AUROC of the UIAS score for 28-day deterioration in ACLF patients was 0.884, indicating an obviously greater predictive performance for the outcomes of ACLF than those of the Child-Pugh (AUROC = 0.646), MELD (AUROC = 0.713), and COSSH-ACLF II scores (AUROC = 0.713). Moreover, we found that heparan sulfate and sulodexide could increase the expression of SDC-1 and attenuate liver injury, by promoting liver regeneration and inhibiting cell apoptosis through the activation of JAK1/STAT3 signalling.

Conclusions Collectively, our findings suggest that SDC-1 represents a potential prognostic and therapeutic target for ACLF and should be further investigated.

Keywords Acute-on-chronic liver failure, Syndecan-1, Heparan sulfate, Sulodexide, Liver regeneration, Cell apoptosis

†Yingli He and Xiaoli Zhang contributed to this paper equally.

*Correspondence:
Yingren Zhao
zhaoyingren@mail.xjtu.edu.cn
Yalei Zhao
ylzhao@xjtu.edu.cn
[1] Department of Infectious Diseases, the First Affiliated Hospital of Xi'an Jiaotong University Medical College, Xi'an, China
[2] National Regional Infectious Diseases Center Co-Constructed By National Health Commission of PRC and People's Government of Shaanxi Province, Xi'an, China
[3] Clinical Medical Research Center of Infectious Diseases, Xi'an, Shaanxi Province, China
[4] Nanfang Hospital, Southern Medical University, Guangzhou, Guangdong Province, China

Background

Acute-on-chronic liver failure (ACLF) is a syndrome characterized by systemic inflammation, and the functional failure of one or more organ systems (liver, kidney, coagulation, brain, respiration, and circulation), in patients with chronic liver disease or cirrhosis [1]. In Asia–Pacific regions, including China, 70–80% of all cases of ACLF are due to hepatitis B virus (HBV) infection (HBV-ACLF) [2]. The mortality rate of ACLF may reach 30–50% at 28 days and 50–80% at 90 days [3–5]. However, a large percentage of ACLF patients may recover from this disorder if timely treatments are provided (e.g., liver transplantation) [5, 6]. Hence, accurate and early prognostic factors and scoring systems are vital to optimize the management of HBV-ACLF [5].

Syndecans constitute a major family of heparan sulfate proteoglycans present on endothelial cells and hepatocytes [7, 8]. Syndecan-1 (SDC-1) is a member of the syndecan family. In the liver, SDC-1 is expressed mainly on hepatocytes and is especially localized at the basolateral surface [9, 10]. SDC-1 is known to act predominantly as a binding partner for integrins or a co-receptor for various growth factors, which regulate various cell behaviors, such as adhesion, invasion, motility, and intracellular signalling [11]. Previous studies have reported that SDC-1 can be shed from the cell surface and produce soluble syndecan ectodomains in both physiological and pathological states [7, 12, 13], which may indicate the prognosis of some diseases. For instance, plasma SDC-1 was significantly increased over 7 days in patients with septic shock, and higher plasma SDC-1 independently predicted 90-day mortality, incident coagulation failure, and the need for renal replacement therapy [14]. Previously, some studies investigated the physiological and pathological functions of SDC-1 in liver diseases. Arnold et al. reported that plasma SDC-1 concentrations in patients with APAP-induced acute liver failure were significantly increased, reaching approximately 2500 ng/ml [15]. SDC-1 may serve as a co-receptor for various growth factors, to activate the phosphorylation of protein kinase B (Akt) and promote liver regeneration, to promoting the phosphorylation of glycogen synthase kinase-3β and reduce hepatocyte apoptosis [7, 16]. However, prior studies have not focused on the correlation between the prognosis of acute liver failure and SDC-1, and this relationship has not been studied in patients with ACLF.

SDC-1 consists of a C-terminal cytoplasmic domain, a transmembrane domain, and an N-terminal ectodomain. The ectodomain connects with three heparan sulfate (HS) chains and two chondroitin sulfate chains [7, 17]. Several studies have reported that the amount of HS present on SDC-1 core proteins regulates both the shedding rate of SDC-1 and the synthesis of core proteins [18, 19].

Sulodexide (SDX) is a heparinoid compound purified from porcine intestinal mucosa that consists of 80% HS and 20% dermatan sulfate [20]. SDX provides material sources for the repair of the glycocalyx, promoting the reconstruction of the glycocalyx and inhibiting the degradation of the glycocalyx [21], contributing to anti-inflammatory, antiaging, antiapoptotic effects, and protecting endothelial cells and the vascular wall in the microcirculation [22]. Huang et al. reported that SDX attenuates liver fibrosis in mice by inhibiting the endothelial-mesenchymal transition of liver sinusoidal endothelial cells [23]. However, the effects of the HS and SDX on ACLF remain to be determined.

In this study, we aim to uncover the prognostic and therapeutic value of SDC-1 in ACLF. First, serum SDC-1 was examined in 2 ACLF cohorts to investigate its potential correlation with short-term mortality in patients with ACLF. Next, we established an ACLF model in mice with carbon tetrachloride (CCl4), lipopolysaccharide (LPS), and D-galactosamine (D-GalN), and did an exploration of the effects of SDX and HS on ACLF in vivo. Our results suggest that serum SDC-1 has prognostic functions in ACLF and that targeting SDC-1 is a potential therapeutic strategy for promoting liver regeneration in ACLF patients.

Methods

Patients and samples

As shown in Fig. 1, two cohorts of ACLF subjects were enrolled. Sample size calculation in the health controls (HCs) and the ACLF group is shown in Additional file 1: 1.1, 34 cases in each group are pretty small in size for our study. We employed a retrospective cohort of 116 ACLF patients for deriving cohort; these patients were referred from April 1, 2019, to June 30, 2023, at admission, and 101 ACLF patients were included for further study. In the second cohort, we enrolled a prospective cohort of 89 ACLF patients for validating cohort; these patients were referred from July 1, 2023, to March 31, 2024, at admission. A total of 73 ACLF patients were included for further study; among them, 36 were HBV-ACLF patients. Moreover, 34 outpatients with chronic hepatitis B (CHB) and 38 with liver cirrhosis who were referred from 1 September 1, 2021, to June 30, 2022, were recruited as pathological controls. In addition, 36 healthy volunteers were included as HCs. All the subjects were recruited or enrolled in the Department of Infectious Disease, First Affiliated Hospital of Xi'an Jiaotong University (Xi'an, China).

The enrolment criteria for patients with ACLF were proposed by the Asian Pacific Association for the Study of the Liver, which defines ACLF as an occurrence of total bilirubin (TBIL) ≥ 5 mg/dL and

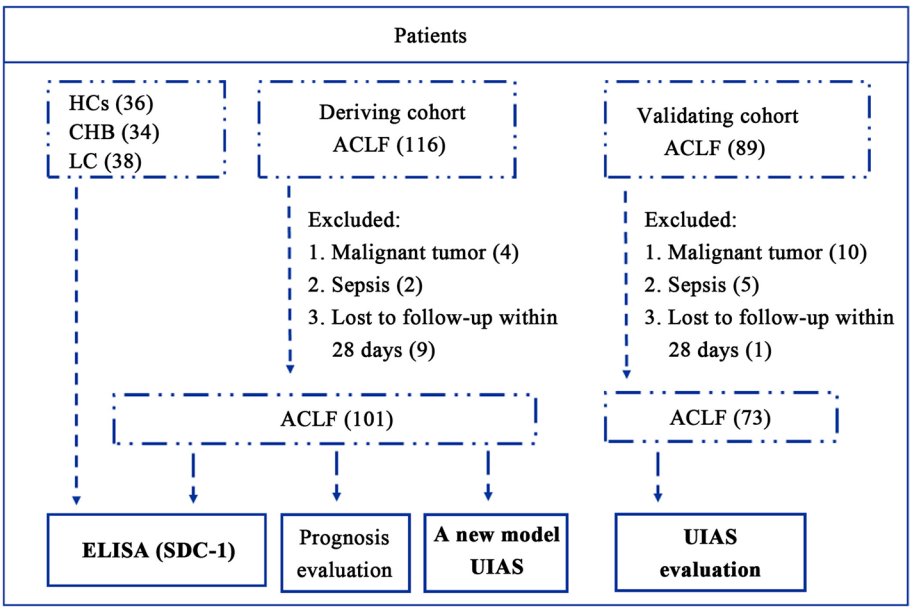

Fig. 1 Enrollment of the patients (HCs, healthy controls; CHB, chronic hepatitis B; LC, liver cirrhosis; ACLF, acute-on-chronic liver failure; SDC-1, syndecan-1; ELISA, enzyme linked immunosorbent assay)

INR ≥ 1.5, concurrent ascites and/or hepatic encephalopathy (HE) within 4 weeks, in patients with or without previously diagnosed chronic liver disease [24]. The enrolment criteria for patients with HBV-ACLF were proposed by the Chinese Group on the Study of Severe Hepatitis B (COSSH-ACLF), and included patients with CHB, TBIL ≥ 12 mg/dL and INR ≥ 1.5, regardless of the presence of cirrhosis [25]. Individuals with malignant tumor or sepsis, and those lost to follow-up were excluded. CHB was defined on the basis of the 2017 guidelines of the European Association for the Study of the Liver (EASL) [26]. The diagnosis of liver cirrhosis was based on the 2021 guidelines of the EASL [27]. Table 1 shows the baseline information of 101 enrolled patients with ACLF in the deriving cohort.

Patients with ACLF were classified into three grades: Grade-1, Grade-2, and Grade-3 (Additional file 1: Table. S1) [25]. Improvement was defined as a decrease of ≥ 1 in the ACLF grade within 28 days after admission. Deterioration was defined as an increase of ≥ 1 in the ACLF grade. Fluctuation was defined as an unchanged grade [28].

All fresh serum samples from the study participants were collected at the First Affiliated Hospital of Xi'an Jiaotong University. The samples were stored in and delivered from the Biobank of the First Affiliated Hospital of Xi'an Jiaotong University.

Enzyme linked immunosorbent assay (ELISA)

Serum SDC-1 levels were measured using a Human SDC-1 ELISA kit (Abcam, USA) and Mouse SDC-1 ELISA kit (CUSABIO, Wuhan, China). Sandwich ELISAs for human and mouse SDC-1 were performed according to the manufacturer's instructions. Human and mice serum in the NC group was not diluted. Serum of patients with ACLF was diluted by 20 × and examined using Human SDC-1 ELISA kit (Abcam, USA). Serum of ACLF mice was diluted by 100 × and examined using Mouse SDC-1 ELISA kit (CUSABIO, Wuhan, China).

A mouse model of ACLF

The mouse model of ACLF is shown in Additional file 1: 1.2.

Protein extraction and western blotting

Protein extraction and western blotting are shown in Additional file 1: 1.3.

Histological analyses and immunofluorescence double-staining

The immunohistochemistry, hematoxylin and eosin (H&E) staining, and immunofluorescence double-staining are shown in Additional file 1: 1.4.

Table 1 Univariate analysis of indicators was performed on the outcome of 101 ACLF patients within 90 days in the deriving cohort

Variables	D90-Survivor ($n=45$)	D90-Non-Survivor ($n=56$)
Clinical characteristics		
Gender		
Male	33 (43.40%)	43 (56.60%)
Female	12 (48.00%)	13 (52.00%)
Age	40.56 ± 11.55	48.75 ± 11.71 ***
HE		
Grade 0	39 (50.60%)	38 (49.40%)
Grade 1	4 (33.30%)	8 (66.70%)
Grade 2	0 (0.00%)	4 (100.00%)
Grade 3	2 (25.00%)	6 (75.00%)
UGIB	2 (15.40%)	11 (54.60%) *
Cirrhosis	33 (38.80%)	52 (61.20%) *
MAP	88.04 ± 11.22	87.76 ± 11.10
Laboratory parameters		
SDC1 (ng/ml)	1106.19 ± 986.64	1670.38 ± 1615.82 *
WBC ($\times 10^9$/L)	5.28 (3.73–8.52)	7.41 (5.31–9.95) *
Lymphocyte	1.10 (0.75–1.42)	0.72 (0.49–1.27) *
Monocyte	0.56 ± 0.36	0.60 ± 0.34
Neutrophil	3.51 (2.51–5.54)	5.71 (3.99–7.44) **
RBC ($\times 10^{12}$/L)	3.82 (3.07–4.21)	3.01 (2.67–3.65) *
Hb (g/L)	117.16 ± 24.93	106.04 ± 24.75 *
PLT ($\times 10^9$/L)	85.00 (52.00–141.00)	69.00 (39.75–101.25)
ALT (U/L)	123.00 (40.50–376.50)	86.00 (41.25–232.75)
AST (U/L)	128.00 (60.50–257.00)	112.00 (56.00–224.25)
TBIL (mg/dL)	13.05 (8.56–19.87)	21.00 (14.44–26.08) ***
TP (g/L)	63.10 (60.00–71.20)	61.55 (54.90–69.23)
ALB (g/L)	31.10 (27.50–33.90)	30.65 (25.20–34.28)
A/G	0.90 (0.79–1.20)	1.00 (0.82–1.30)
ALP (U/L)	139.00 (118.00–203.50)	146.50 (113.25–200.75)
GGT (U/L)	71.00 (42.00–98.00)	52.50 (41.00–107.00)
CHE (U/L)	2769.00 (2321.50–3702.00)	3249.50 (1815.75–4367.25)
INR	1.87 (1.68–2.46)	2.46 (1.91–2.96) ***
K (mmol/L)	3.73 (3.38–3.99)	4.02 (3.47–4.45)
Na (mmol/L)	137.40 (134.35–140.95)	134.00 (131.55–136.90) **
Cr (mg/dL)	0.62 (0.50–0.72)	0.68 (0.51–0.96)
BUN (mmol/L)	4.35 (3.21–6.29)	5.74 (4.07–8.03) *
CPT	11.00 (10.00–12.00)	12.00 (11.00–13.00) ***
COSSH-ACLF II	6.77 ± 0.97	7.96 ± 0.98 ***
MELD	19.19 ± 6.75	25.90 ± 8.38 ***

UGIB upper gastrointestinal bleeding, *MAP* mean arterial pressure, *WBC* white blood cell, *RBC* red blood cell, *Hb* hemoglobin, *PLT* Platelet, *ALT* alanine aminotransferase, *AST* aspartate aminotransferase, *TP* Total protein, *ALB* albumin, *A/G* albumin/globulin, *ALP* alkaline phosphatase, *GGT* gamma-glutamyl transpeptidase, *CHE* cholinesterase, *K* Potassium, *Na* Sodium, *Cr* creatinine, *BUN* blood urea nitrogen, *CPT* Child-Pugh rating

**P < 0.05, **P < 0.01, ***P < 0.001*

Proteomics, protein–protein interaction (PPI) network construction, and enrichment analysis

Three biological replicates from each group were used for the proteomic experiments. The mass spectrometry proteomics data have been deposited to the ProteomeXchange Consortium (https://proteomecentral.proteomexchange.org) via the iProX partner repository with the dataset identifiers PXD059999/IPX0010236001. The interaction network among the differentially expressed proteins between the ACLF group and the ACLF+SDX group or ACLF+HS group was constructed using the STRING database (https://cn.string-db.org/) [29]. Visualization of the PPI networks

were achieved with the Cytoscape 3.9.1 software. Cluster analysis was performed using the M-code in the Cytoscape 3.9.1 software. Gene Ontology (GO) and Kyoto Encyclopedia of Genes and Genomes (KEGG) pathway enrichment analyses were performed using the Vishenon platform (https://www.bioinformatics.com.cn/) [30] and the Majorbil cloud platform (https://www.majorbio.com/) [31].

Scoring models

The Child-Pugh score was calculated in the basis of TBIL, serum albumin, prothrombin time, ascites, and the HE score [32]. The MELD score was calculated using the following formula: MELD = 3.78 × ln (TBIL, mg/dL) + 11.2 × ln (INR) + 9.57 × ln (serum creatinine, mg/dL) + 6.4 × (etiological index, alcoholic or biliary is 0; the others are 1) [33]. The COSSH-ACLF II score was calculated as: COSSH-ACLF II = 1.649 × ln (INR) + 0.457 × HE score + 0.425 × ln (neutrophil count, 10^9/L) + 0.396 × ln (TBIL, μmol/L) + 0.576 × ln (blood urea, mmol/L) + 0.033 × age (year) [25].

Statistical analysis

GraphPad Prism 8.0.1 (GraphPad Software Inc., San Diego, California, USA) and SPSS 27.0 (SPSS, Inc., Chicago, IL) software were used. A two-tailed $P < 0.05$ was considered significant. Continuous data were expressed as medians ± standard errors or medians with interquartile ranges (P25—P75). Comparisons of data between groups were performed using Student's *t* test or the nonparametric Mann–Whitney *U* test. Categorical data were calculated as numbers (%) and were compared by chi-squared test or Fisher's exact test. We included individual factors ($P < 0.15$) to identify independent prognostic factors for HBV-ACLF with multivariate Cox regression analysis. A correlation analysis was performed using the Pearson tests. Cumulative survival rates were determined via the Kaplan-Meier method. Orthogonal partial least squares-discriminant analysis (OPLS-DA) was used to rank the prognostic performance of the parameters in HBV-ACLF patients using SIMCA 14.1 software (Umetrics AB, Umea, Sweden). In addition, non-normally distributed factors were $\log_2$-transformed. The UIAS prognostic model was developed based on multivariate logistic regression. The areas under the ROC (AUROCs) curve of the prognostic scoring systems were compared via the *Z*-test using Delong's method.

Results

Serum SDC-1 was elevated in patients with ACLF, and higher baseline serum SDC-1 levels indicated a poor prognosis for patients with ACLF

As shown in Fig. 2A, the baseline serum SDC-1 levels were significantly higher in 101 patients with ACLF (847.72, 499.79–1511.37 ng/ml) than in 38 patients with liver cirrhosis (93.84, 59.16–129.02 ng/ml), 34 patients with CHB infection (36.16, 28.00–62.40 ng/ml) and 36 HCs (33.58, 27.08–43.34 ng/ml) (all $P < 0.0001$).

We further explored whether the serum SDC-1 level could serve as a novel prognostic biomarker for ACLF. Correlations between serum SDC-1 levels and several clinical indicators were analyzed. The serum SDC-1 levels were moderately correlated with TBIL ($r = 0.528$, $P = 0.000$), aspartate aminotransferase (AST, $r = 0.435$, $P = 0.000$), neutrophils ($r = 0.418$, $P = 0.000$), and MELD scores ($r = 0.409$, $P = 0.000$) (as shown in Fig. 2B). These values were slightly correlated with alanine transaminase (ALT, $r = 0.371$, $P = 0.000$), red blood cells (RBCs, $r = 0.336$, $P = 0.001$), creatinine (Cr, $r = 0.309$, $P = 0.002$), and the COSSH-ACLF II score ($r = 0.336$, $P = 0.001$) (Additional file 1: Fig. S1A).

According to our 28-day and 90-day clinical observations, the baseline SDC-1 levels of patients who died or accepted a liver transplantation (LT) within 90 days were markedly greater than those of patients who survived ($P < 0.05$) (Table 1 and Fig. 2C). The AUROC of SDC-1 for 90-day mortality was 0.588, with a sensitivity of 0.536 and specificity of 0.644 at an optimum cutoff value of 917.420 ng/ml. According to that, patients in the deriving cohort were divided into a higher SDC-1 group (SDC-1 > 917.420 ng/ml) or a lower SDC-1 group (SDC-1 ≤ 917.420 ng/ml). The survival rate of the lower SDC-1 group was significantly greater than that of the higher SDC-1 group ($P = 0.039$) (Fig. 2D). The serum SDC-1 level in patients who died or accepted a LT within 28 days had an increased tendency compared to patients who survived (Fig. 2E). Thus, according to 28-day observations, the patients were further divided into 3 groups (improvement, fluctuation, and deterioration). We found that patients who showed deterioration (1359.36, 675.08–4096.97 ng/ml) had higher baseline serum SDC-1 levels than did patients who improved (845.13, 609.78–1459.75 ng/ml) ($P = 0.034$; Fig. 2F).

A novel prognostic model (UIAS) was developed to predict the prognosis of ACLF patients based on SDC-1

In 38 ACLF patients who achieved improvement and 24 patients who showed deterioration, OPLS-DA was used to rank the ability of the indicators to predict the prognosis of ACLF patients (Fig. 3A,B). As shown in Fig. 3A, 29 clinical and laboratory parameters could better distinguish patients with improvement from patients with deterioration. The top 5 predictors with little variability between the 2 groups were $\lg_2$ (SDC-1), $\lg_2$ (TBIL), $\lg_2$ (INR), $\lg_2$ (albumin), and $\lg_2$ (total protein) (Fig. 3B). The test permutation indicated that the model fits well (Additional file 1: Fig. S1B).

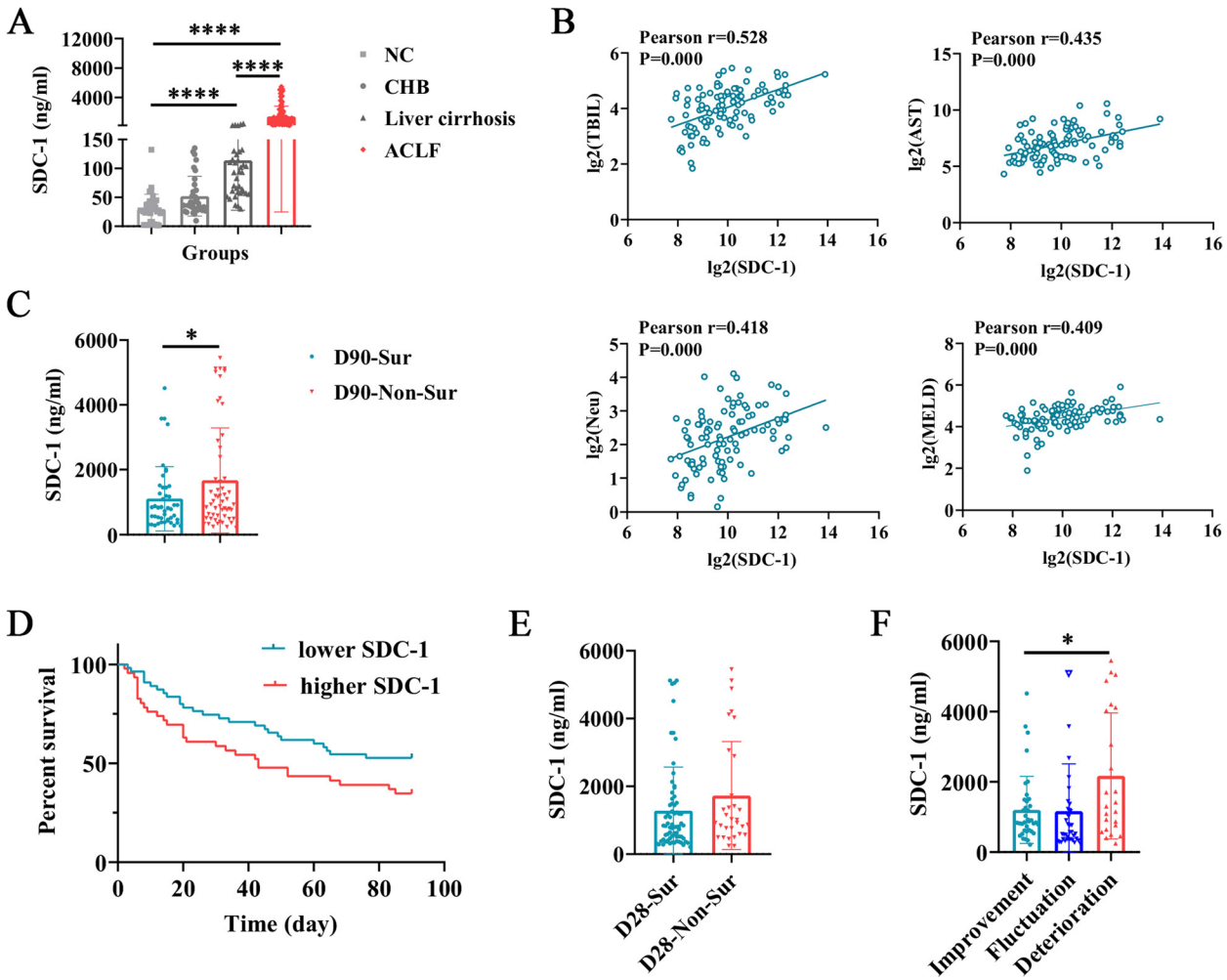

Fig. 2 SDC-1 was dysregulated in patients with ACLF, and higher baseline serum SDC-1 levels indicated a poor prognosis in ACLF patients. **A** Baseline serum SDC-1 levels in 101 patients with ACLF, 38 patients with liver cirrhosis, 34 patients with CHB and 36 HCs. **B** Correlations between the serum SDC-1 level and total bilirubin (TBIL), aspartate aminotransferase (AST), neutrophil (Neu), and the MELD score. **C** Baseline SDC-1 levels of patients who died or accepted a LT within 90 days (D90-Non-Sur, $n=56$) and patients who survived (D90-Sur, $n=45$). **D** Survival rate of ACLF patients in the lower SDC-1 group ($n=55$) and higher SDC-1 group ($n=46$). **E** Baseline SDC-1 levels of patients who died or accepted a LT within 28 days (D28-Non-Sur, $n=31$) and patients who survived (D28-Sur, $n=70$). **F** Baseline SDC-1 levels of patients in the improvement ($n=38$), fluctuation ($n=39$), and deterioration groups ($n=24$) within 28 days. $^{*}P<0.05$, $^{****}P<0.0001$

Univariate analysis was performed to assess the influence of clinical and laboratory indicators on the outcome of ACLF (Table 1 and Additional file 1: Table. S3). Multivariate Cox regression revealed that age, upper gastrointestinal bleeding (UGIB), SDC-1, and the INR were independent prognostic predictors in ACLF patients (all $P<0.05$, Table 2). Thus, age, UGIB, SDC-1, and the INR were ultimately identified as potential prognostic indicators. A novel prognostic model (UIAS) was developed as follows: $\text{UIAS}=0.076\times\text{Age}+0.001\times\text{SDC-1}+1.454\times\text{INR}+2.854\times\text{UGIB}-12.165$. UGIB = 1 for patients without UGIB, and 2 for patients with UGIB.

The UIAS score was strongly associated with the MELD and COSSH-ACLF II scores ($r=0.588$, and 0.629, respectively; all $P=0.000$), and positively associated with the Child-Pugh score ($r=0.238$, $P=0.016$; Additional file 1: Fig. S2A). The AUROC of the UIAS score for 28-day deterioration in ACLF patients was 0.884, with a sensitivity of 0.833 and a specificity of 0.868 at a cut-off value of −0.174 (Fig. 3C). Compared with the Child-Pugh (AUROC = 0.646), MELD (AUROC = 0.713), and COSSH-ACLF II scores (AUROC = 0.713), the UIAS clearly had greater predictive performance for the outcomes of ACLF (Fig. 3C). The AUROC of the UIAS score for 90-day mortality in ACLF patients was 0.800, with a sensitivity of 0.804 and a specificity of 0.689 at a cut-off value of −1.515, which was similar to that of the COSSH-ACLF II score (Fig. 3D). According to the optimum cut-off

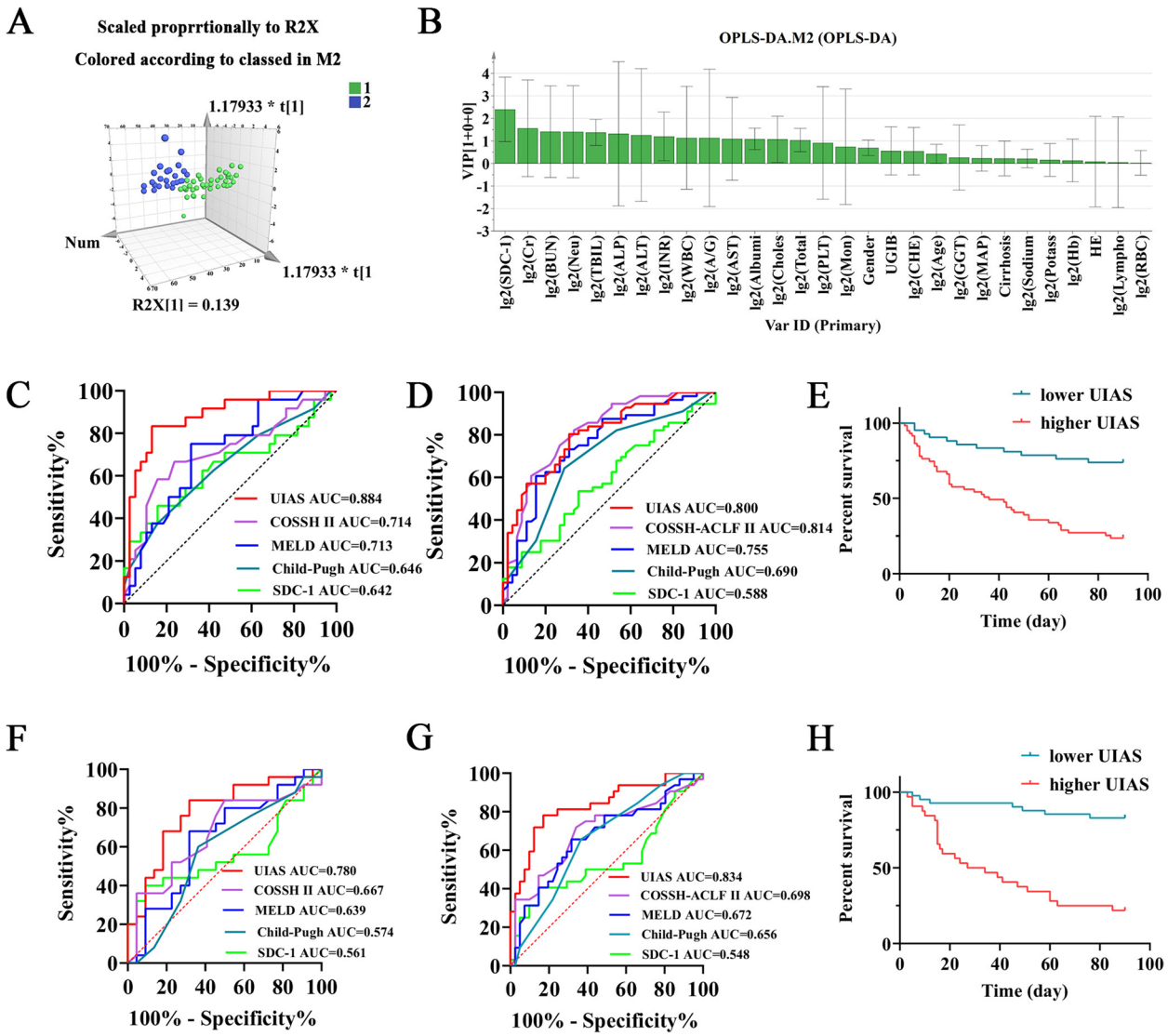

Fig. 3 Development and evaluation of a new model to predict the prognosis of ACLF patients based on SDC-1. **A**,**B** OPLS—DA was used to rank the ability of the indicators to predict the prognosis of ACLF patients. **C** AUROCs of the UIAS score, COSSH-ACLF II score, MELD score, and Child-Pugh score for 28-day deterioration in ACLF patients in the deriving cohort. **D** AUROCs of the UIAS score, COSSH-ACLF II score, MELD score, and Child-Pugh score for 90-day mortality in ACLF patients in the deriving cohort. **E** Survival rate of ACLF patients in the lower UIAS score group and higher UIAS score group in the deriving cohort. **F** AUROCs of the UIAS score, COSSH-ACLF II score, MELD score, and Child-Pugh score for 28-day deterioration in ACLF patients in the validating cohort. **G** AUROCs of the UIAS score, COSSH-ACLF II score, MELD score, and Child-Pugh score for 90-day mortality in ACLF patients in the validating cohort. **H** Survival rate of ACLF patients in the lower UIAS score group and higher UIAS score group in the validating cohort

value, patients in the deriving cohort were divided into a higher UIAS group (UIAS score > −1.515) or a lower UIAS group (UIAS score ≤ −1.515). The survival rate of the lower UIAS group was significantly greater than that of the higher UIAS group ($P < 0.0001$) (Fig. 3E). The UIAS score in the non-survivor group within 90 days was significantly greater than that in the survivor group in the driving cohort ($P < 0.0001$; Additional file 1: Fig. S2B).

The validating cohort included 73 ACLF patients for further study (Fig. 1). Baseline information about the patients was shown in Table. S4. The AUROC of the UIAS score for 28-day deterioration in ACLF patients was 0.780, which showed obviously higher predictive performance than did the Child-Pugh (AUROC = 0.574), MELD (AUROC = 0.639), and COSSH-ACLF II scores (AUROC = 0.667) (Fig. 3F). The AUROC of the UIAS score for 90-day mortality was 0.834, which showed obviously higher predictive performance than did the Child-Pugh (AUROC = 0.656), MELD (AUROC = 0.672), and COSSH-ACLF II scores (AUROC = 0.698) (Fig. 3G).

Table 2 Multivariate Cox regression analysis of indicators associated with the deterioration of ACLF patients within 28 days

Variables in the equation								
	B	S.E	Wald	df	Sig	Exp (B)	95% CI for Exp (B)	
							Lower	Upper
Age	0.076	0.035	4.758	1	0.029	1.079	1.008	1.155
UGIB	2.854	1.125	6.432	1	0.011	17.358	1.912	157.546
SDC-1	0.001	0.000	6.226	1	0.013	1.001	1.000	1.001
INR	1.454	0.480	9.186	1	0.002	4.281	1.672	10.963
Constant	−12.165	3.113	15.272	1	0.000	0.000		

Because 70–80% of all Chinese ACLF cases are attributable to HBV infection, we further analyzed 36 HBV-ACLF patients in a validating cohort conforming to the COSSH-ACLF criteria. The AUROC of the COSSH-ACLF II score significantly increased, and the AUROCs of the UIAS score for 28-day deterioration and 90-day mortality in HBV-ACLF patients were 0.897 and 0.859, respectively, which showed higher predictive ability than COSSH-ACLF II scores (0.869 and 0.786, respectively) (Additional file 1: Fig. S3A, C). The survival rate of the lower UIAS group (UIAS score ≤ −2.737) in the validating cohort was significantly greater than that of the higher UIAS group (UIAS score > −2.737) (Fig. 3H).

A mouse model of ACLF was established

To establish a mouse model of ACLF, we used CCl4, D-GalN, and LPS to induce a liver injury to mimic the disease progression of ACLF (Fig. 4A). Serum ALT and AST levels of the ACLF mice were significantly increased (Fig. 4B). Transmission electron microscopy (TEM) revealed that necrotic hepatocytes and significantly swollen mitochondria were presented in the livers of the mice in the ACLF group, the cristae of the mitochondria were lost (Fig. 4C). H&E staining images and corresponding semiquantitative analysis showed that the mice in ACLF group presented severe hepatic necrosis and inflammatory infiltration (Fig. 4D, E). The apoptotic hepatocytes were stained with a commercial Tunel staining kit, and the results showed that the positive staining area was increased in the ACLF mice (Fig. 4D, E), which indicated increased cell apoptosis. Moreover, we observed an increased number of $F4/80^+$ macrophages and MPO^+ neutrophils in the mice with ACLF, which supported more severe hepatic inflammation in those mice than in the NC mice (Fig. 4D, E). In addition, the Masson dying results showed that hepatic fibrosis was exacerbated in the livers of the mice treated with CCl4 for 8 weeks compared with those of the NC mice (Additional file 1: Fig. S4). As a result, we believe that a mouse model of ACLF was successfully established and characterized by hepatocellular injury, exacerbated inflammation, and hepatic fibrosis.

SDX and HS attenuated ACLF by promoting liver regeneration and suppressing cell apoptosis

The ACLF + SDX group were administered with SDX once a day by gastric gavage for 1 month in ACLF mice (Fig. 5A). The mice in the ACLF + HS group were intraperitoneally injected with HS 1 h before the administration of D-GalN and LPS (Fig. 5B). According to the TEM results, the livers of the mice with ACLF presented with apoptotic hepatocytes at different stages, and severely swollen mitochondria. In contrast, the livers from the ACLF + SDX and ACLF + HS groups had only slightly swollen mitochondria, and there was no hepatocellular apoptosis (Fig. 5C). Semiquantitative analysis of H&E staining inflammatory and necrotic scores showed that SDX and HS significantly alleviated liver injury in the mice with ACLF (Fig. 5D).

Compared with those in the NC group, the levels of serum SDC-1 were markedly increased in the ACLF group (Fig. 6A), which was consistent with the serum SDC-1 levels in ACLF patients (Fig. 2A). As shown in Fig. 6B, SDC-1 was expressed primarily on hepatocytes and the hepatic sinusoid in healthy mouse livers, but expressed decreased (Fig. 6C) and was distributed in a disordered manner (Fig. 6B) in the livers of the ACLF mice. Furthermore, SDX and HS decreased the downregulation of SDC-1 and decreased the expression of cytokeratin 18 (CK18) in ACLF mice (Fig. 6B, C), suggesting that SDX and HS attenuated liver injury probably by decreasing the reduction of SDC-1.

To explore the possible mechanisms by which SDX and HS improve liver injury, we detected liver regeneration indicators by examining cyclin D1, cyclin E1, and proliferating cell nuclear antigen (PCNA), and examined hepatocyte apoptotic parameters by performing Cleaved-caspase3 (C-caspase3), Caspase3, Bcl2, and Bax in the 4 groups. In the liver tissues of the ACLF group, cyclin D1, and cyclin E1 were downregulated,

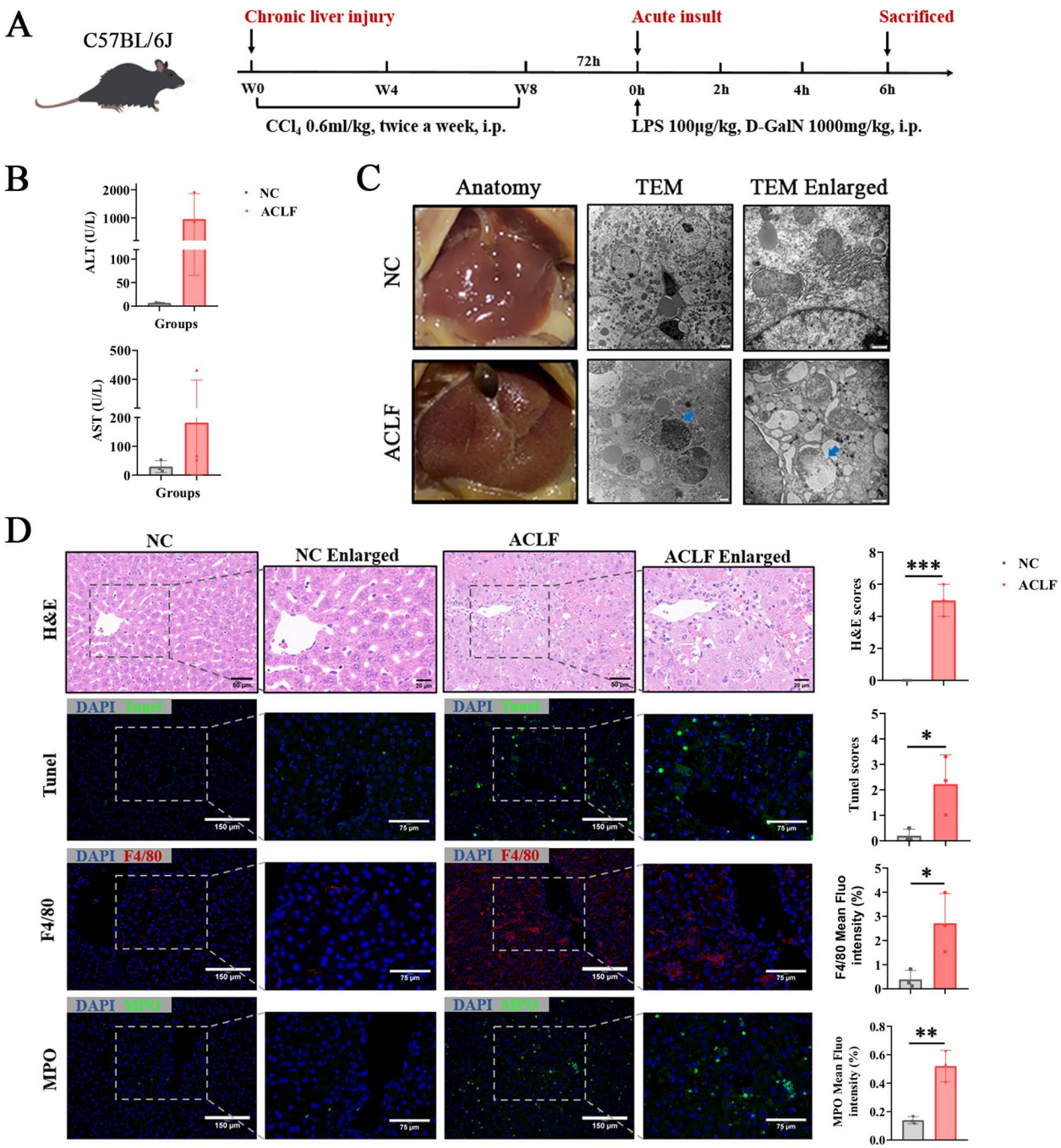

Fig. 4 An ACLF mouse model was developed. **A** Mice in the ACLF group were intraperitoneally injected with a mixture of carbon tetrachloride (CCl4) and olive oil twice a week for 8 weeks. At 72 h after the last injection, the mice were intraperitoneally injected with D-galactosamine (D-GalN, 1000 mg/kg) and lipopolysaccharide (LPS, 100 μg/kg), and sacrificed after 6 h. **B** Levels of serum alanine transaminase (ALT) and AST in the mice were examined. **C** Livers of the mice were observed via transmission electron microscopy (TEM). The blue arrows in this image represent necrotic hepatocytes and severely swollen mitochondria. The scales are respectively 2 μm and 500 nm. **D, E** Representative images of hematoxylin and eosin (H&E) staining, Tunel staining, F4/80 staining, and MPO staining of liver sections from the indicated mice. The corresponding semiquantitative data of the staining among the groups are shown. The scales used for H&E staining are respectively 50 and 20 μm. The scales used for Tunel staining, F4/80 staining, and MPO staining are respectively 150 and 75 μm. $^{*}P < 0.05$, $^{**}P < 0.01$, $^{***}P < 0.001$

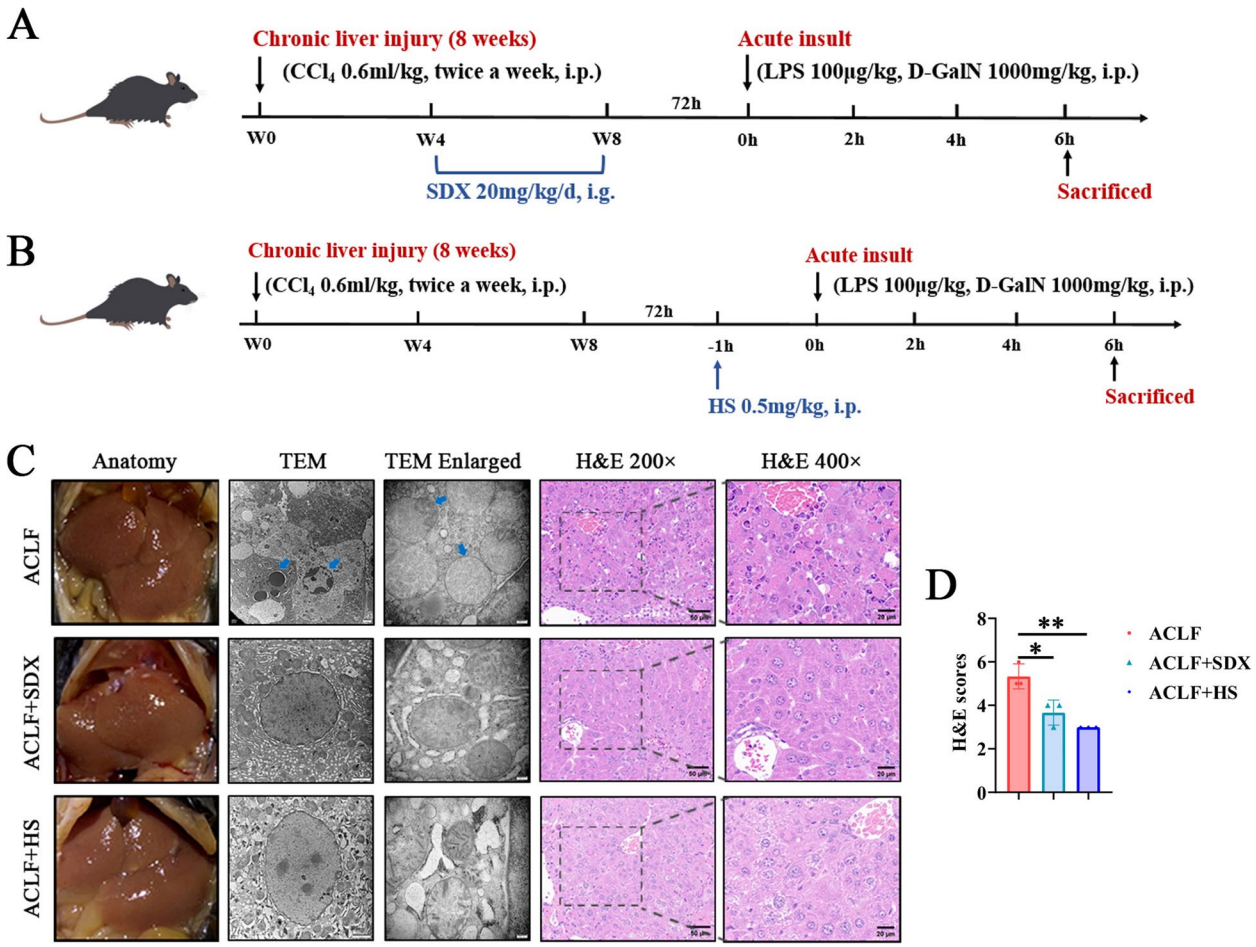

Fig. 5 SDX and HS attenuated liver injury in an ACLF mouse model. **A** ACLF mice (induced similarly to those in Group 2) were administered with sulodexide (SDX, 20 mg/kg/day) by gastric gavage once a day for 1 month. **B** ACLF mice (induced similarly in Group 2) were intraperitoneally injected with heparan sulfate (HS, 0.5 mg/kg) 1 h before the administration of D-GalN and LPS. **C** Representative images of TEM images and H&E staining of liver sections from the indicated mice. In TEM, the blue arrows in this image respectively represent late and early apoptotic liver cells, and severely swollen mitochondria. The scales in the TEM images are respectively 2 μm and 200 nm. The scales used for H&E staining are respectively 50 and 20 μm. **D** Corresponding semiquantitative data of H&E-stained inflammatory and necrotic scores among the groups. $^{*}P < 0.05$, $^{**}P < 0.01$

Bcl2/Bax was downregulated, and C-caspase3 was upregulated compared with those in the NC group (Fig. 6C, D). However, SDX and HS increased the expression of cyclin D1, cyclin E1, and Bcl2/Bax, and decreased the expression of C-caspase3 in the ACLF mice (Fig. 6C, D). A large number of $PCNA^{+}$ hepatocytes were detected in the NC, ACLF + SDX, and ACLF + HS livers, whereas the ACLF group had a much smaller number of $PCNA^{+}$ hepatocytes (Fig. 6E). The above data indicate that liver regeneration was suppressed with significant hepatocyte apoptosis in the ALCF mice and that SDX and HS obviously increased liver regeneration and reduced cell apoptosis in the mice with ACLF.

SDX and HS promoted liver regeneration and exerted anti-apoptotic effects, likely through the JAK1/STAT3 signalling pathways

We next performed proteomics to investigate the possible mechanisms responsible for the promotion of liver regeneration and reduction in apoptosis by SDX and HS. We searched for 315 differentially expressed proteins in the ACLF + SDX group compared with the ACLF group (Fig. 7A, B), and 336 differentially expressed proteins in the ACLF + HS group compared with the ACLF group (Fig. 7D, E). We subsequently identified 132 proteins that were differentially expressed in both the ACLF + SDX group and the ACLF + HS group (Additional file 1: Fig. S5A). For

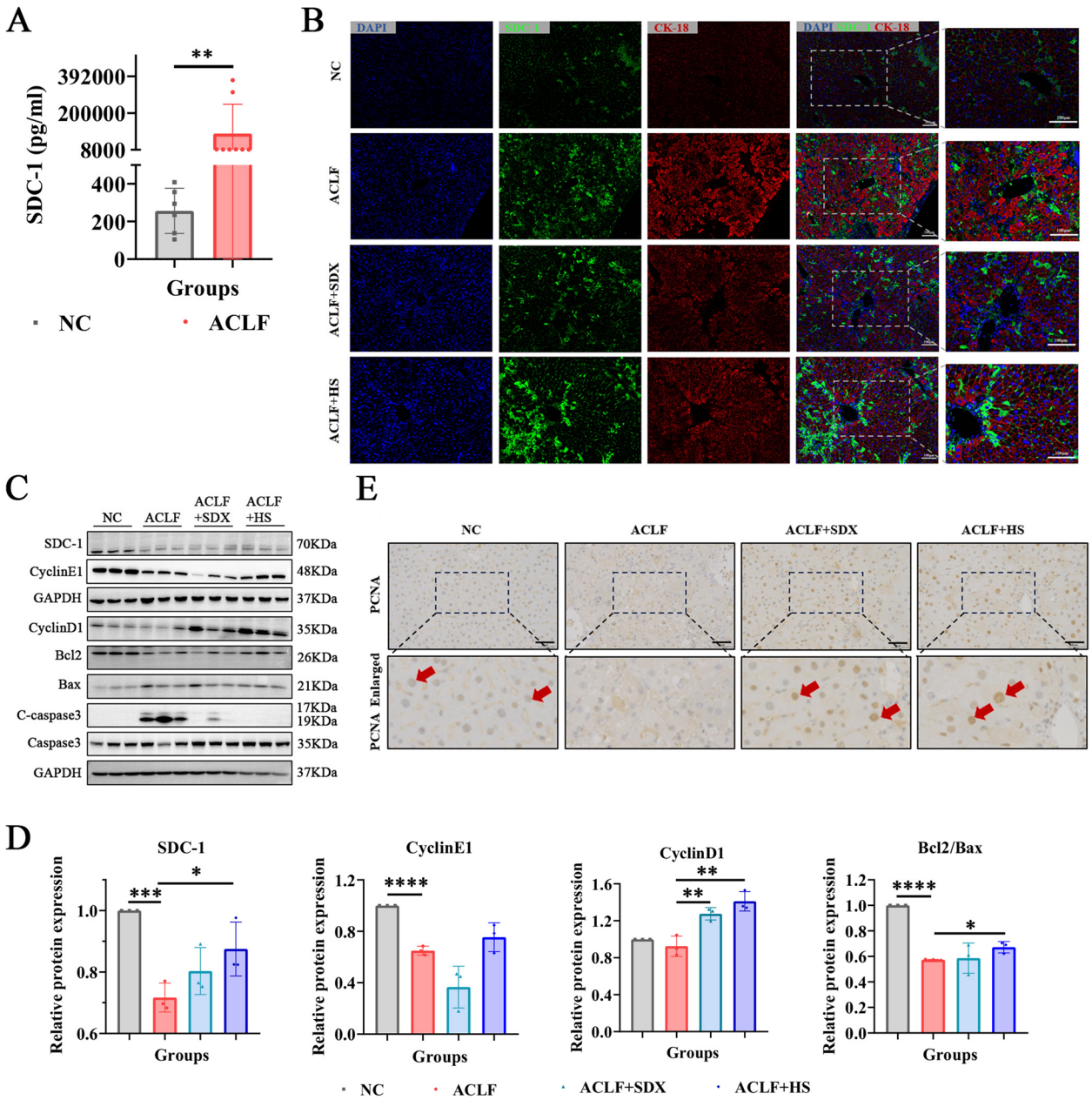

Fig. 6 SDX and HS inhibited the degradation of SDC-1, promoted liver regeneration, and suppressed liver apoptosis. **A** Serum SDC-1 levels of the mice in the NC and ACLF groups. **B** The expression of SDC-1 and cytokeratin 18 (CK-18) was performed by immunofluorescence double-staining. The scale is 100 μm. **C**, **D** Protein expression levels of SDC-1, indicators of cell proliferation (Cyclin D1, Cyclin E1 and PCNA), and cell apoptosis (Bcl2/Bax, C-caspase3) were examined by western blotting in liver tissues from the 4 groups. **E** PCNA expression was examined by immunohistochemistry, and the red arrows represent the PCNA$^+$ hepatocytes. The scale is 50 μm.$^*P<0.05$, $^{**}P<0.01$, $^{***}P<0.001$, $^{****}P<0.0001$

these 132 proteins, a PPI network was constructed using STRING (https://cn.string-db.org/) [29] and Cytoscape (Additional file 1: Fig. S5B). GO and KEGG analyses were conducted using the Vishenon platform (https://www.bioinformatics.com.cn/) [30] and the Majorbil cloud platform (https://www.majorbio.com/) [31] (Additional file 1: Fig. S5C-D).

Differentially expressed proteins between the ACLF+SDX and ACLF groups, and between the ACLF+HS and ACLF groups were further analyzed. For differentially expressed proteins in the ACLF+SDX group, the PPI network clusters are shown in Additional file 1: Fig. S5E-F. The KEGG analysis results showed that the cAMP signalling, TGF-beta signalling, and MAPK signalling pathways were enriched (Fig. 7C).

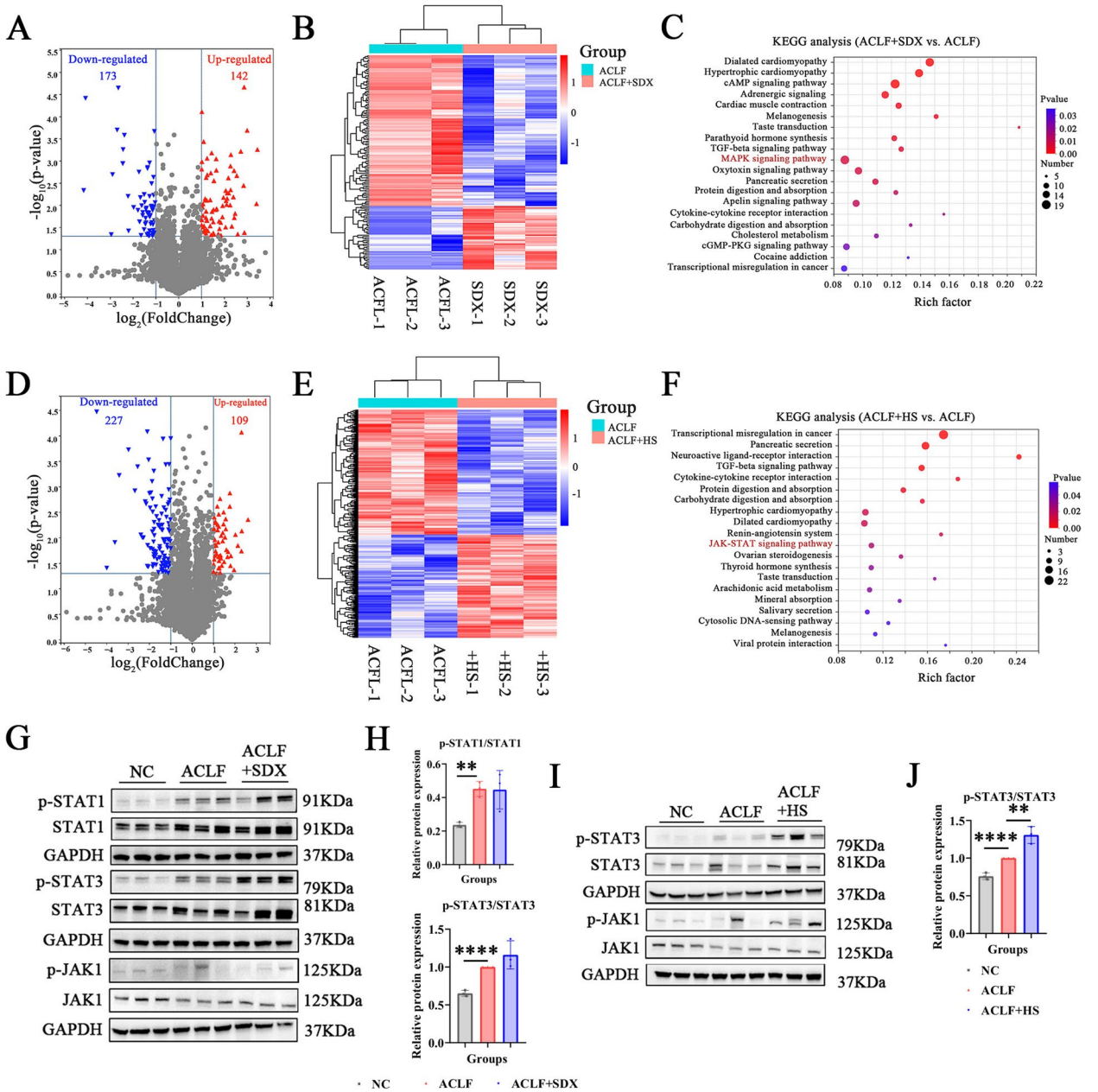

Fig. 7 SDX and HS promoted liver regeneration and exerted anti-apoptotic effects, likely through the JAK1/STAT3 signalling pathway. **A,B** A total of 315 differentially expressed proteins were identified via volcano plots and heat maps in the ACLF + SDX mice compared with the ACLF mice. **C** KEGG analysis results of the 315 differentially expressed proteins in the ACLF + SDX mice compared with the ACLF mice. **D, E** A total of 336 differentially expressed proteins were identified via volcano plots and heat maps in the ACLF + HS mice compared with the ACLF mice. **F** KEGG analysis results of the 336 differentially expressed proteins in the ACLF + HS mice compared with the ACLF mice. **G, H** Protein-expression levels of p-STAT1/STAT1, p-STAT3/STAT3, and p-JAK1/JAK1 in liver tissues. **I, J** Protein-expression levels of p-STAT3/STAT3 and p-JAK1/JAK1 in liver tissues $^{**}P < 0.01$, $^{****}P < 0.0001$

For the differentially expressed proteins in the ACLF + HS group, the PPI network clusters are shown in Fig. S5G. The KEGG analysis results showed that the TGF-beta signalling and JAK/STAT signalling pathways were enriched (Fig. 7F). The JAK/STAT and MAPK pathways were reportedly to be involved in the activation of anti-apoptotic and proliferation-promoting signalling in hepatocytes. Among them, STAT3 is a key anti-apoptotic factor that alleviates liver injury through the upregulation of the antiapoptotic proteins Bcl2 [34–36]. Next, we examined the phosphorylation

levels of P38-MAPK in the 4 groups using western blotting. We found no significant changes in the phosphorylation level of P38-MAPK between the ACLF+SDX group and the ACLF group, or between the ACLF+HS group and the ACLF group (Additional file 1: Fig. S6). We subsequently examined the phosphorylation level of JAK/STAT. We found that phosphorylation levels of both STAT1 and STAT3 were elevated in the ACLF group compared with those in the NC group (Fig. 7G, H). SDX increased the phosphorylation level of JAK1/STAT3 in ACLF mice (Fig. 7G, H). Similarly, HS also induced the activation of JAK1/STAT3 in ACLF mice (Fig. 7I, J), indicating that SDX and HS promote liver regeneration and exert anti-apoptotic effect probably through the JAK1/STAT3 pathways.

Discussion

At present, many researchers have attempted to optimize the prognostic scorings of ACLF with the aim of identifying biomarkers that are already or not yet applied in clinical practice. These biomarkers include metabolic markers [5, 37, 38], liver functional reserve biomarkers [39, 40], and inflammatory biomarkers [41]. There was a microcirculation disturbance (hepatic microcirculation was impaired) in liver injury or failure [42, 43]. However, few studies have identified biomarkers related to microcirculation disturbances to evaluate their diagnostic, prognostic, and therapeutic effects. Piotti et al. reported that plasma SDC-1 was significantly increased in patients with endothelial damage in septic shock, and increased plasma SDC-1 independently predicted the 90-day mortality, the need for renal replacement therapy, and incident coagulation failure [14]. In this study, we found that baseline serum SDC-1 levels could serve as a novel prognostic factor for patients with ACLF.

In Asia–Pacific regions, including China, 70–80% of all patients with ACLF have HBV-ACLF [2]. Patients with CHB without rational treatment can develop liver fibrosis, liver cirrhosis, or even ACLF. Thus, we examined serum SDC-1 levels in HCs and in patients with CHB, liver cirrhosis, and ACLF. We found that the serum SDC-1 levels in patients with CHB, liver cirrhosis, and ACLF were elevated compared with those in HCs, especially in ACLF patients. Our study aimed to evaluate the prognostic value of serum SDC-1 levels in ACLF patients, and whether SDC-1 can also be used as a biomarker for CHB and LC needs to be studied further.

Moreover, 29 clinical and laboratory indicators were thoroughly analyzed using two separate methods (Cox regression and OPLS-DA) in our study (Table 2 and Fig. 3B). Among these factors, age, UGIB, SDC-1, and the INR were identified as the four best factors for predicting 28-day deterioration. Interestingly, the OPLS-DA model between the improvement and deterioration groups demonstrated that TBIL was one of the top 5 powerful predictors, but Cox regression revealed that it was not an independent predictor for the prognosis of ACLF. Furthermore, SDC-1 and TBIL were strongly correlated (Fig. 2B), suggesting that SDC-1 is likely an indicator replacing TBIL in the prediction of 28-day deterioration in patients with ACLF. We developed a simpler prognostic model (UIAS) for ACLF, which was superior to the Child-Pugh, MELD, and COSSH-ACLF scores for the prediction of 28-day deterioration, and at least comparable with the COSSH-ACLF score for the prediction of 90-day mortality.

In our study, we employed a retrospective cohort of 116 ACLF patients for deriving cohort from April 1, 2019, to June 30, 2023, at admission. In the second cohort, we enrolled a prospective cohort of 89 ACLF patients for the validating cohort, who were referred from July 1, 2023, to March 31, 2024, at admission. The serum of patients in the deriving cohort was stored longer than that of patients in the validating cohort was, but the UIAS prognostic model developed in the deriving cohort was still applicable to the validating cohort. The model needs to be validated in other clinical centers in the future.

Our study revealed that SDC-1 expression is decreased in the livers of mice with liver injury induced by LPS+D-GalN and that the serum SDC-1 is increased in patients and mice with ACLF. Several studies have reported that SDC-1 can be shed from the cell surface and produce soluble syndecan ectodomains in both physiological and pathological states [7, 12, 13, 44]. Accordingly, whether SDC-1 is shed from liver tissues to the microcirculation after liver injury needs further exploration in the future.

As a transmembrane protein, the ectodomain of SDC-1 connects with three HS chains [7, 17]. Several studies have reported that the amount of HS present on SDC-1 core proteins regulates both the shedding rate of SDC-1 and the synthesis of core proteins [18, 19, 45, 46]. SDX is a heparinoid compound that consists of 80% HS [20]. Some studies have demonstrated that SDX provides material sources for the repair of the glycocalyx and inhibits its degradation [21, 47]. Our study revealed that SDX and HS decreased the degradation of SDC-1, and attenuated liver injury by promoting liver regeneration and inhibiting liver apoptosis (Fig. 6). SDC-1 is known to act primarily as a co-receptor for various growth factors, which regulate some cell behaviors, such as adhesion, invasion, and motility [11, 48]. Hence, SDX and HS promote liver regeneration and inhibit liver apoptosis likely by decreasing the degradation of SDC-1.

STAT3 plays crucial roles in hepatocarcinogenesis by inhibiting apoptosis and promoting cell cycle progression [49]. The biological functions of STAT1 include

inhibiting cell growth and promoting cell apoptosis [50]. Xiang et al. reported that IL-6/STAT3 was blocked, and IFN-γ/STAT1 was activated in mice with ACLF induced by CCl4 and *Klebsiella pneumoniae*, thereby attenuating liver regeneration [51]. Our study revealed that STAT3 and STAT1 were both activated in a mouse model of ACLF induced by CCl4, LPS, and D-GalN, liver regeneration was ultimately inhibited and apoptosis occurred in ACLF. Thus, STAT1 was probably strongly activated (represented by the bold red arrow in Fig. 8), STAT3 was weakly activated (thin black arrow in Fig. 8), liver regeneration was ultimately inhibited, and apoptosis occurred in ACLF. SDX and HS promote liver regeneration and exert anti-apoptotic effects through the activation of STAT3 (as shown in Fig. 8). SDC-1 is known to act predominantly as a binding partner for integrins or a co-receptor for various growth factors [11]. The ectodomain of SDC-1 connects with three HS chains and two chondroitin sulfate chains [7, 17]. HS may activate the JAK1/STAT3 pathway may through the interaction of cytokine receptors, such as growth factors. However, the part described in the dotted box in Fig. 8 needs to be studied further in vitro experiments in the future. Nam et al. reported that SDC-1 serves as a co-receptor for growth factors to phosphorylate Akt and promote liver regeneration [16]. In the future, on the basis of our study, overexpression or knockdown of SDC-1 in vivo and vitro is needed to show its effect on ACLF through JAK/STAT pathways.

There are some limitations in the present study. First, this was a single-center study, and the sample size of this study was limited. The prognostic UIAS score should be validated in multi-center and cross-sectional cohorts in the future. Second, the mechanisms by which SDX and HS modulate the activity of the JAK/STAT pathways need to be further investigated. Third, bacterial infections occur in up to two-thirds of ACLF patients and contribute to poor clinical outcomes [51]. The mouse ACLF model used in this study could only partially mimic the pathological characteristics of ACLF patients. Therefore, another liver injury model involving the combination of CCl4 injection and bacterial infection (*Klebsiella pneumoniae*) is needed to validate our findings in the future, to increase the clinical translational potential of this study.

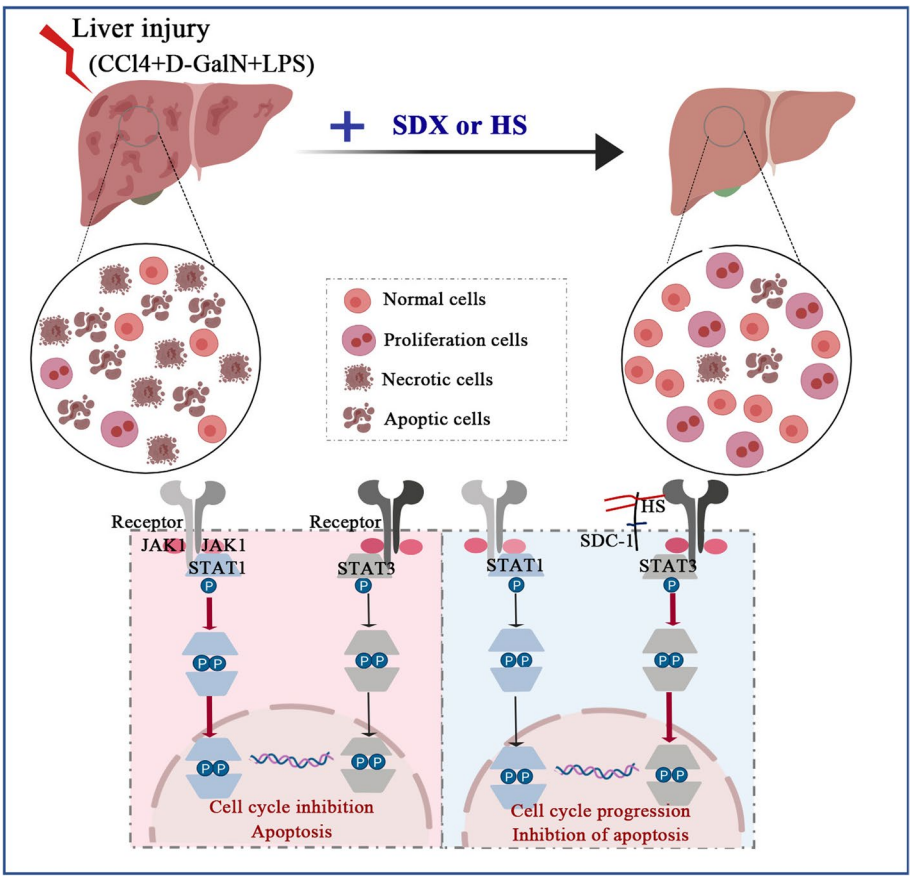

Fig. 8 Schematic diagram. SDX and HS alleviated liver injury by promoting liver regeneration and inhibiting liver apoptosis. SDX and HS promote liver regeneration and exert anti-apoptotic effects, probably by activating the JAK1/STAT3 pathways

Conclusions

In summary, the present study demonstrated that the expression of SDC-1 in liver tissues was reduced, and that soluble SDC-1 in the microcirculation was increased in ACLF. Baseline serum SDC-1 levels could serve as a novel prognostic factor for patients with ACLF. The novel prognostic model (UIAS) showed obviously greater predictive performance for the outcomes of ACLF than did the Child-Pugh, MELD, and COSSH-ACLF II scores. SDX and HS promoted liver regeneration through the JAK1/STAT3 pathway.

Abbreviations

ACLF	Acute-on-chronic liver failure
HBV	Hepatitis B virus
SDC-1	Syndecan-1
Akt	Protein kinase B
HS	Heparan sulfate
SDX	Sulodexide
CCl4	Carbon tetrachloride
LPS	Lipopolysaccharide
D-GalN	D-galactosamine
CHB	Chronic hepatitis B
REDCap	Research Electronic Data Capture
TBIL	Total bilirubin
HE	Hepatic encephalopathy
COSSH-ACLF	Chinese Group on the Study of Severe Hepatitis B
EASL	European Association for the Study of the Liver
ELISA	Enzyme-linked immunosorbent assay
H&E	Hematoxylin and eosin
PPI	Protein-protein interaction
GO	Gene ontology
KEGG	Kyoto Encyclopedia of Genes and Genomes
OPLS-DA	Orthogonal partial least squares-discriminant analysis
AUROC	Area under the ROC curve
HCs	Healthy controls
AST	Aspartate aminotransferase
ALT	Alanine transaminase
RBC	Red blood cell
Cr	Creatinine
LT	Liver transplantation
UGIB	Upper gastrointestinal bleeding
TEM	Transmission electron microscope
CK18	Cytokeratin 18
PCNA	Proliferating cell nuclear antigen
C-caspase3	Cleaved-caspase3
MAP	Mean arterial pressure

Supplementary Information

The online version contains supplementary material available at https://doi.org/10.1186/s12916-025-03931-4.

Additional file 1. Additional File 1: 1—Methods. Additional File 1: 2—Tables S1—S4. Table S1—Grades of ACLF patients. Table S2—The primary antibodies for western blotting. Table S3—A univariate analysis of indicators plays on the deterioration of ACLF patients within 28 days in the deriving cohort. Table S4—A univariate analysis of clinical and laboratory indicators plays on the outcome of 73 ACLF patients within 90 days in the validating cohort. Additional File 1: 3—Figures S1—S6. Figure S1—(A) Correlations between serum SDC-1 levels and several clinical indicators. (B) The OPLS-DA test permutation indicated that the model fits well. Figure S2—(A) Correlations between UIAS score and other ACLF scores. (B) The UIAS score in ACLF patients of the non-survivor group and survivor group within 90 days in the driving cohort. Figure S3—The AUROC of the UIAS score, COSSH-ACLF II, MELD, and Child-Pugh score respectively for 28-day deterioration, 28-day mortality and 90-day mortality in validating cohort of 36 HBV-ACLF patients. Figure S4—Masson dying in livers of NC group and mice treated by CCl4 for 8 weeks. Figure S5—Venn map, PPI network, GO and KEGG analyses of differential proteins between ACLF + SDX and ACLF group, ACLF + HS and ACLF group. Figure S6—Phosphorylation level of P38-MAPK in 4 groups.

Additional file 2.

Acknowledgements

The study was supported by the Clinical Research Award of the First Affiliated Hospital of Xi'an Jiaotong University, China (No. 2022-XKCRC-04), and Biobank of the First Affiliated Hospital of Xi'an Jiaotong University, China.

Authors' contributions

Y.Z1., Y.H., and X.Z. designed the research. Y.H. and X.Z. wrote the main manuscript text. Y.Y1., J.L1., T.N., Q.Z., and Y.L. enrolled the patients and collected clinical samples. X.Z., S.F., and Y.F. collected the clinical data and followed up the patients. S.F., R.W., and T.N. designed and performed the experiments in vivo. X.Z. analyzed the data and prepared Figs. 1, 2, 3, 4, 5, and 6. Y.H. and Y.Z1. prepared Figs. 7–8. Z.L., J.L2., Y.Y2., and Y.Z2. provided essential material and technical guidance. Y.Z1. and Y.Z2. revised the manuscript. Y.H. and X.Z. contributed equally to this work. All authors read and approved the final manuscript.

Funding

This work was funded by the Fundamental Research Funds for the Central Universities (xzy012023111), National Natural Science Foundation of China Grants (82070641), and the Institutional Foundation of the First Affiliated hospital of Xi'an Jiaotong University (2021QN-05).

Data availability

The datasets used and/or analysed during the current study are available from the corresponding author on reasonable request.

Declarations

Ethics approval and consent to participate

This work was conducted in compliance with the principles of the 1975 Declaration of Helsinki and was approved by the Ethics Committee of the First Affiliated Hospital of Xi'an Jiaotong University (XJTU1AF2023LSK-019). We obtained written consent form all study participants.

Consent for publication

All of the anonymous information were entered into a secure Research Electronic Data Capture (REDCap) system, and are available from the corresponding author on reasonable request.

Competing interests

The authors declare no competing interests.

Received: 4 September 2024 Accepted: 6 February 2025
Published online: 21 February 2025

References

1. Moreau R, Tonon M, Krag A, Angeli P, Berenguer M, Berzigotti A, et al. EASL clinical practice guidelines on acute-on-chronic liver failure. J Hepatol. 2023;79(2):461–91.
2. Hernaez R, Solà E, Moreau R, Ginès P. Acute-on-chronic liver failure: an update. Gut. 2017;66(3):541–53.
3. Shi Y, Yang Y, Hu Y, Wu W, Yang Q, Zheng M, et al. Acute-on-chronic liver failure precipitated by hepatic injury is distinct from that precipitated by extrahepatic insults. Hepatology. 2015;62(1):232–42.
4. Jalan R, Saliba F, Pavesi M, Amoros A, Moreau R, Ginès P, et al. Development and validation of a prognostic score to predict mortality in patients with acute-on-chronic liver failure. J Hepatol. 2014;61(5):1038–47.

5. Wu D, Sun Z, Liu X, Rao Q, Chen W, Wang J, et al. HINT: a novel prognostic model for patients with hepatitis B virus-related acute-on-chronic liver failure. Aliment Pharmacol Ther. 2018;48(7):750–60.
6. Shawcross DL, Austin MJ, Abeles RD, McPhail MJW, Yeoman AD, Taylor NJ, et al. The impact of organ dysfunction in cirrhosis: Survival at a cost? J Hepatol. 2012;56(5):1054–62.
7. Bernfield M, Götte M, Park PW, Reizes O, Fitzgerald ML, Lincecum J, et al. Functions of cell surface heparan sulfate proteoglycans. Annu Rev Biochem. 1999;68(1):729–77.
8. Baghy K. Proteoglycans in liver cancer. World J Gastroenterol. 2016;22(1):379.
9. Roskams T, Moshage H, De Vos R, Guido D, Yap P, Desmet V. Heparan sulfate proteoglycan expression in normal human liver. Hepatology. 1995;21(4):950–8.
10. Weiner OH, Zoremba M, Gressner AM. Gene expression of syndecans and betaglycan in isolated rat liver cells. Cell Tissue Res. 1996;285(1):11–6.
11. Couchman JR. Transmembrane signaling proteoglycans. Annu Rev Cell Dev Biol. 2010;26(1):89–114.
12. Jalkanen M, Rapraeger A, Saunders S, Bernfield M. Cell surface proteoglycan of mouse mammary epithelial cells is shed by cleavage of its matrix-binding ectodomain from its membrane-associated domain. J Cell Biol. 1987;105(6):3087–96.
13. Wang Z, Götte M, Bernfield M, Reizes O. Constitutive and accelerated shedding of murine syndecan-1 is mediated by cleavage of its core protein at a specific juxtamembrane site. Biochemistry. 2005;44(37):12355–61.
14. Piotti A, Novelli D, Meessen JMTA, Ferlicca D, Coppolecchia S, Marino A, et al. Endothelial damage in septic shock patients as evidenced by circulating syndecan-1, sphingosine-1-phosphate and soluble VE-cadherin: a substudy of ALBIOS. Crit Care. 2021;25(1):113.
15. Arnold K, Xu Y, Sparkenbaugh EM, Li M, Han X, Zhang X, et al. Design of anti-inflammatory heparan sulfate to protect against acetaminophen-induced acute liver failure. Sci Transl Med. 2020;12(535):eaav8075.
16. Nam EJ, Hayashida K, Aquino RS, Couchman JR, Kozar RA, Liu J, et al. Syndecan-1 limits the progression of liver injury and promotes liver repair in acetaminophen-induced liver injury in mice. Hepatology. 2017;66(5):1601–15.
17. Reszegi A, Tátrai P, Regős E, Kovalszky I, Baghy K. Syndecan-1 in liver pathophysiology. Am J Physiol Cell Physiol. 2022;323(2):C289–94.
18. Ramani VC, Pruett PS, Thompson CA, Delucas LD, Sanderson RD. Heparan sulfate chains of syndecan-1 regulate ectodomain shedding. J Biol Chem. 2012;287(13):9952–61.
19. Mahtouk K, Hose D, Raynaud P, Hundemer M, Jourdan M, Jourdan E, et al. Heparanase influences expression and shedding of syndecan-1, and its expression by the bone marrow environment is a bad prognostic factor in multiple myeloma. Blood. 2007;109(11):4914–23.
20. Masola V, Zaza G, Onisto M, Lupo A, Gambaro G. Glycosaminoglycans, proteoglycans and sulodexide and the endothelium: biological roles and pharmacological effects. Int Angiol. 2014;33(3):243–54.
21. Broekhuizen LN, Lemkes BA, Mooij HL, Meuwese MC, Verberne H, Holleman F, et al. Effect of sulodexide on endothelial glycocalyx and vascular permeability in patients with type 2 diabetes mellitus. Diabetologia. 2010;53(12):2646–55.
22. Tarbell JM, Cancel LM. The glycocalyx and its significance in human medicine. J Intern Med. 2016;280(1):97–113.
23. Huang R, Deng J, Zhu C-P, Liu S-Q, Cui Y-L, Chen F, et al. Sulodexide attenuates liver fibrosis in mice by restoration of differentiated liver sinusoidal endothelial cell. Biomed Pharmacother. 2023;160:114396.
24. Sarin SK, Kedarisetty CK, Abbas Z, Amarapurkar D, Bihari C, Chan AC, et al. Acute-on-chronic liver failure: consensus recommendations of the Asian Pacific Association for the Study of the Liver (APASL) 2014. Hepatol Int. 2014;8(4):453–71.
25. Wu T, Li J, Shao L, Xin J, Jiang L, Zhou Q, et al. Development of diagnostic criteria and a prognostic score for hepatitis B virus-related acute-on-chronic liver failure. Gut. 2018;67(12):2181–91.
26. Lampertico P, Agarwal K, Berg T, Buti M, Janssen HLA, Papatheodoridis G, et al. EASL 2017 Clinical Practice Guidelines on the management of hepatitis B virus infection. J Hepatol. 2017;67(2):370–98.
27. European Association for the Study of the Liver. EASL clinical practice guidelines on non-invasive tests for evaluation of liver disease severity and prognosis - 2021 update. J Hepatol. 2021;75(3):659–89.
28. Wang J, Zhang X, Han J, Zhou P, Yu X, Shen Z, et al. MicroRNA-124 expression in Kupffer cells modulates liver injury by targeting IL-6/STAT3 signaling. Antiviral Res. 2023;211: 105510.
29. Szklarczyk D, Kirsch R, Koutrouli M, Nastou K, Mehryary F, Hachilif R, et al. The STRING database in 2023: protein–protein association networks and functional enrichment analyses for any sequenced genome of interest. Nucleic Acids Res. 2023;51(D1):D638–46.
30. Tang D, Chen M, Huang X, Zhang G, Zeng L, Zhang G, et al. SRplot: a free online platform for data visualization and graphing. PLoS ONE. 2023;18(11):e0294236.
31. Ren Y, Yu G, Shi C, Liu L, Guo Q, Han C, et al. Majorbio Cloud: A one-stop, comprehensive bioinformatic platform for multiomics analyses. iMeta. 2022;1(2):e12.
32. Cholongitas E, Papatheodoridis GV, Vangeli M, Terreni N, Patch D, Burroughs AK. Systematic review: The model for end-stage liver disease–should it replace Child-Pugh's classification for assessing prognosis in cirrhosis? Aliment Pharmacol Ther. 2005;22(11–12):1079–89.
33. Kamath PS, Kim WR. The model for end-stage liver disease (MELD). Hepatology. 2007;45(3):797–805.
34. Lei Z, Yu J, Wu Y, Shen J, Lin S, Xue W, et al. CD1d protects against hepatocyte apoptosis in non-alcoholic steatohepatitis. J Hepatol. 2024;80(2):194–208.
35. Yuan F-H, Chen Y-L, Zhao Y, Liu Z-M, Nan C-C, Zheng B-L, et al. microRNA-30a inhibits the liver cell proliferation and promotes cell apoptosis through the JAK/STAT signaling pathway by targeting SOCS-1 in rats with sepsis. J Cell Physiol. 2019;234(10):17839–53.
36. Shen W, Chen C, Guan Y, Song X, Jin Y, Wang J, et al. A pumpkin polysaccharide induces apoptosis by inhibiting the JAK2/STAT3 pathway in human hepatoma HepG2 cells. Int J Biol Macromol. 2017;104(Pt A):681–6.
37. Zhang Y, Tan W, Wang X, Zheng X, Huang Y, Li B, et al. Metabolic biomarkers significantly enhance the prediction of HBV-related ACLF occurrence and outcomes. J Hepatol. 2023;79(5):1159–71.
38. Juanola A, Graupera I, Elia C, Piano S, Solé C, Carol M, et al. Urinary L-FABP is a promising prognostic biomarker of ACLF and mortality in patients with decompensated cirrhosis. J Hepatol. 2022;76(1):107–14.
39. Wu D, Zhang S, Xie Z, Chen E, Rao Q, Liu X, et al. Plasminogen as a prognostic biomarker for HBV-related acute-on-chronic liver failure. J Clin Invest. 2020;130(4):2069–80.
40. Baldassarre M, Naldi M, Zaccherini G, Bartoletti M, Antognoli A, Laggetta M, et al. Determination of effective albumin in patients with decompensated cirrhosis: clinical and prognostic implications. Hepatology. 2021;74(4):2058–73.
41. Hassan HM, Liang X, Xin J, Lu Y, Cai Q, Shi D, et al. Thrombospondin 1 enhances systemic inflammation and disease severity in acute-on-chronic liver failure. BMC Med. 2024;22(1):95.
42. Zhang Y, Huber P, Praetner M, Zöllner A, Holdt L, Khandoga A, et al. Serine proteases mediate leukocyte recruitment and hepatic microvascular injury in the acute phase following extended hepatectomy. Microcirculation. 2023;30(1): e12796.
43. La Mura V, Pasarín M, Rodriguez-Vilarrupla A, García-Pagán JC, Bosch J, Abraldes JG. Liver sinusoidal endothelial dysfunction after LPS administration: a role for inducible-nitric oxide synthase. J Hepatol. 2014;61(6):1321–7.
44. Hayashida K, Bartlett AH, Chen Y, Park PW. Molecular and cellular mechanisms of ectodomain shedding. Anat Rec. 2010;293(6):925–37.
45. Jung O, Trapp-Stamborski V, Purushothaman A, Jin H, Wang H, Sanderson RD, et al. Heparanase-induced shedding of syndecan-1/CD138 in myeloma and endothelial cells activates VEGFR2 and an invasive phenotype: prevention by novel synstatins. Oncogenesis. 2016;5(2):e202.
46. Yang Y, Macleod V, Miao H-Q, Theus A, Zhan F, Shaughnessy JD, et al. Heparanase enhances syndecan-1 shedding: a novel mechanism for stimulation of tumor growth and metastasis. J Biol Chem. 2007;282(18):13326–33.
47. Schött U, Solomon C, Fries D, Bentzer P. The endothelial glycocalyx and its disruption, protection and regeneration: a narrative review. Scand J Trauma Resusc Emerg Med. 2016;24(1):48.
48. Theocharis AD, Skandalis SS, Tzanakakis GN, Karamanos NK. Proteoglycans in health and disease: novel roles for proteoglycans in malignancy and their pharmacological targeting. FEBS J. 2010;277(19):3904–23.

49. Park H, Lee S, Lee J, Moon H, Ro SW. Exploring the JAK/STAT signaling pathway in hepatocellular carcinoma: unraveling signaling complexity and therapeutic implications. Int J Mol Sci. 2023;24(18):13764.
50. Hu X, Li J, Fu M, Zhao X, Wang W. The JAK/STAT signaling pathway: from bench to clinic. Signal Transduct Target Ther. 2021;6(1):402.
51. Xiang X, Feng D, Hwang S, Ren T, Wang X, Trojnar E, et al. Interleukin-22 ameliorates acute-on-chronic liver failure by reprogramming impaired regeneration pathways in mice. J Hepatol. 2020;72(4):736–45.

Publisher's Note